ACS OMEGA

Article

Cite This: ACS Omega 2019, 4, 21251−21259

http://pubs.acs.org/journal/acsodf

Synthesis and Photoluminescence of Tetracyanidonitridorhenium(V) Complexes with Five-Membered N-Heteroaromatic Ligands and Photoluminescence-Intensity Change

Moe Seike,[†] Kojiro Nagata,[‡] Hayato Ikeda,[†] Akitaka Ito,[§] Eri Sakuda,[∥] Noboru Kitamura,[⊥] Atsushi Shinohara,[†,#] and Takashi Yoshimura*[,‡,#]

[†]Department of Chemistry, Graduate School of Science, Osaka University, Toyonaka 560-0043, Japan

[‡]Radioisotope Research Center, Institute for Radiation Sciences, Osaka University, Suita 565-0871, Japan

[§]Major of Molecular Design, School of Environmental Science and Engineering, Kochi University of Technology, Kochi 782-8502, Japan

[∥]Division of Chemistry and Materials Science, Graduate School of Engineering, Nagasaki University, Nagasaki 852-8521, Japan

[⊥]Department of Chemical Sciences and Engineering, Graduate School of Chemical Sciences and Engineering, Hokkaido University, Sapporo 060-0810, Japan

[#]Project Research Center for Fundamental Sciences, Graduate School of Science, Osaka University, Toyonaka 560-0043, Japan

Supporting Information

ABSTRACT: Novel tetracyanidonitridorhenium(V) complexes with five-membered N-heteroaromatic ligands, $(PPh_4)_2[ReN(CN)_4L]$ [L = imidazole (Him) (**2**), 1-methylimidazole (Mim) (**3**), and pyrazole (pyz) (**4**)] and $(PPh_4)_2[ReN(CN)_4L]\cdot L$ [L = Him (**5**) and Mim (**6**)], were synthesized by the reactions of $(PPh_4)_2[ReN(CN)_4]$ (**1**) with Him, Mim, and pyz, and their structures were determined by single-crystal X-ray analysis. The complexes **2**, **3**, **4**, and **6** showed intense photoluminescence, with the emission quantum yields (Φ_{em}) being 0.65−0.75 in the solid state at 296 K. In contrast, the Φ_{em} and τ_{em} values of **5** are significantly smaller and shorter, respectively, than the relevant values of **2**. The interconversion reactions among **1**, **2**, and **5** accompanied by large photoluminescence-intensity changes were accomplished by solvent-free reactions and exposure of water. The mechanochemical reaction of **2** with 1 mol equiv of Him in the solid state gave **5**. Complex **5** was also obtained by the mechanochemical reaction of **1** with 2 mol equivalents of Him in the solid state. By placing solid of **5** in water, the solid showed intense photoluminescence to give **2**. Complex **1** was produced under vacuum at 185 °C from **2** or **5**.

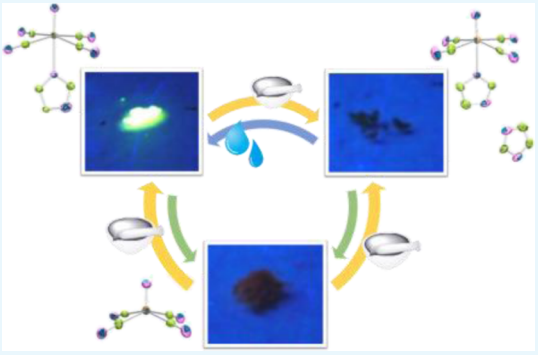

INTRODUCTION

A reversible photoluminescence intensity on−off by external stimuli and/or by a chemical reaction is attractive with respect to development of sensing. It is a promising approach to apply a weak interaction to construct the switch using a reversible chemical reaction. Metal complexes have an advantage to be capable to use a weak coordination bond as well as a hydrogen bond and an intermolecular interaction for this purpose. We suppose that the control of the on−off reaction using the weak interaction/bond in a solid state is sometimes easier than that in a solution because thermal motion of the molecule is restricted in the solid state. In practice, the reversible luminescence color and/or intensity switching of metal complexes via mechanochemical reactions have been studied extensively for d^{10} and d^8 complexes.[1−44] The driving force of luminescence intensity change in these complexes was by change in intermolecular interactions such as the $\pi-\pi$ interaction. In contrast, the solid-based reversible reactions involving drastic luminescence intensity change by change in the coordination number and composition of the complex are still rare.

A nitridorhenium(V) complex possesses a coordination site (axial site) at the trans position of the nitrido, and the site is influenced strongly by the trans effect of the nitrido.[45−48] Therefore, the site is labile, the sixth ligand is not necessary, and the five- and six-coordinate complexes are both stable.[49] In addition, some types of the both five- and six-coordinate complexes show luminescence.[49−58] In the

Received: August 26, 2019
Accepted: October 22, 2019
Published: November 4, 2019

DOI: 10.1021/acsomega.9b02749
ACS Omega 2019, 4, 21251−21259

tetracyanidonitridorhenium(V) complex, the emission quantum yield of the five-coordinate complex is low (Φ_{em} < 0.01) and, thus, the complex is almost nonemissive by naked eyes.[49] The six-coordinate complex shows intense luminescence in the solid state at 296 K.[49,58] Therefore, the luminescence on−off reaction using the weak coordination site is promising for the complex. We previously reported vapochromic luminescence of soild tetracyanidonitridorhenium(V) by the changes in the coordination number and coordinating volatile organic compounds such as acetone, acetonitrile, ethanol, and methanol.[49]

In the present study, the new nitridorhenium(V) complexes with five-membered N-heteroaromatic ligands, imidazole (Him), *N*-methylimidazole (Mim), and pyrazole (pyz) as shown in Figure 1 were synthesized and characterized to

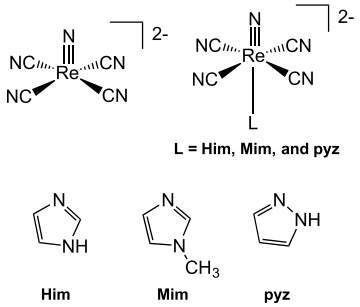

Figure 1. Structures of $[ReN(CN)_4]^{2-}$ and $[ReN(CN)_4L]^{2-}$ (L = Him, Mim, and pyz).

investigate luminescence on−off properties for the tetracyanidonitridorhenium(V) complex by changes in weak interactions. In the complexes having Him and Mim, we succeeded in synthesizing two types of crystalline samples depending on the reaction conditions: six-coordinate complexes and also complexes including the additional one mole ratio of the N-heterocyclic molecule. Most newly synthesized complexes showed strong luminescence in the solid states at 296 K. Interestingly, we found that the Him-coordinated complex including one mole ratio of noncoordinating Him in the crystal was almost nonluminescent, while the Mim-coordinated complex containing one mole ratio of noncoordinating Mim in the crystal was strongly photoemissive. Luminescence-intensity changes between the five- and six-coordinate complexes and between the six-coordinate complexes with Him were investigated based on solvent-free mechanochemical and vacuum elimination reactions and an exposure of water to the solid complex. The origin of the luminescence intensity change is both formation/dissociation of weak interactions and the coordination bond between tetracyanidonitridorhenium(V) and Him.

RESULTS AND DISCUSSION

Synthesis and Characterization of the Novel Complexes. The new bright yellow-green luminescent six-coordinate complexes, $(PPh_4)_2[ReN(CN)_4Him]$ (**2**) and $(PPh_4)_2[ReN(CN)_4Mim]$ (**3**), were synthesized by the reactions of $(PPh_4)_2[ReN(CN)_4]$ (**1**) with excess five-membered N-heterocyclic ligands in water. The reaction of **1** with an excess amount of pyz in CH_2Cl_2 gave $(PPh_4)_2[ReN(CN)_4pyz]$ (**4**) in a high yield. The similar reaction of **1** with an excess amount of Him or Mim in CH_2Cl_2 produced the six-coordinate complex coordinated with the Him or Mim ligand which occupies at the axial site of the nitridorhenium(V) complex. In $(PPh_4)_2[ReN(CN)_4Him]\cdot Him$ (**5**) or $(PPh_4)_2[ReN(CN)_4Mim]\cdot Mim$ (**6**), furthermore, additional one mole ratio of noncoordinate Him or Mim was included. In the infrared (IR) spectra, the absorption bands ascribed to the N-heterocyclic ligands were observed in addition to those of the $(PPh_4)^+$ and $[ReN(CN)_4]^{2-}$ units, as shown in the Supporting Information, Figure S1. The ^1H NMR spectra of the new complexes dissolved in CD_3CN showed the signals of N-heterocyclic ligands and $(PPh_4)^+$. Each integral signal intensity ratio of the N-heterocycle to $(PPh_4)^+$ was 1:2 for **2**, **3**, or **4** and 1:1 for **5** or **6**. These ratios were in good agreement with the results of the single-crystal X-ray analyses of the complexes. In **5** and **6**, one set of the ^1H NMR signals of Him and Mim was only observed, suggesting that the dissociation of Him and Mim ligands from the rhenium ion rapidly occurred in the solutions as the result of strong trans effect of the nitrido. The single-crystal X-ray structures of the new complexes were determined. The crystal structures of the complex anions of **2**, **3**, **4**, **5**, and **6** are displayed in Figure 2. The crystallographic data of the new complexes are shown in Table S1. The structures and selected bond distances/angles of the new complexes are summarized in Table 1. Each complex anion has a distorted octahedral structure with one nitrido atom being located at the axial site and an N-heteroaromatic ligand being occupied at the trans site to the nitrido. The four cyanido ions coordinate at the equatorial positions with the Re−C bond distances of 2.094(3)−2.128(6) Å and the N(nitrido)≡Re−C angles of 96.41(10)−101.32(19)°. The bond distance of Re≡N(nitrido) is in the range of 1.659(4)−1.671(4) Å. The Re−C and Re≡N(nitrido) bond distances are similar to those of the previously reported tetracyanidonitridorhenium(V) complexes.[49,58−61] The N-

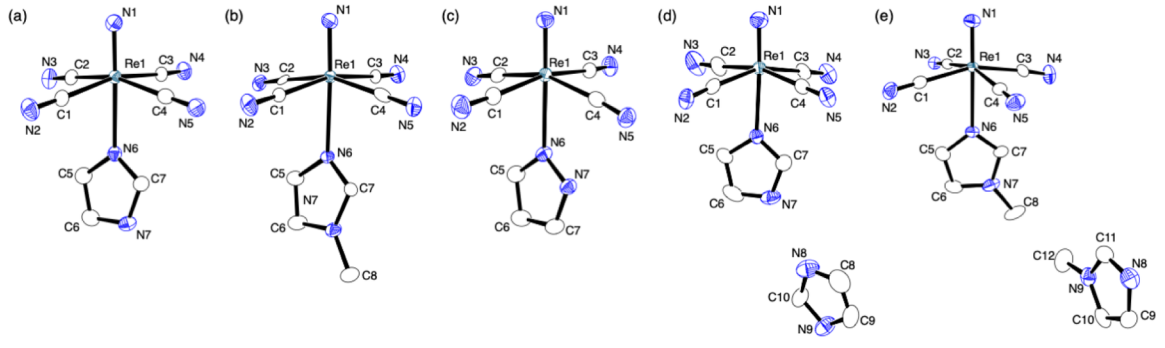

Figure 2. ORTEP drawings of the complex anions of **2** (a), **3** (b), **4** (c), **5** (d), and **6** (e). Hydrogen atoms are omitted for clarity.

DOI: 10.1021/acsomega.9b02749
ACS Omega 2019, 4, 21251−21259

Table 1. Selected Bond Distances (Å) and Angles (deg) of the Tetracynidonitridorhenium(V) Complexes with Five-Membered N-Heterocyclic Ligands

	2	3	4	5	6
			Bond Distances		
Re≡N	1.664(2)	1.663(5)	1.668(2)	1.659(4)	1.671(4)
Re−C	2.106(3)−2.116(3)	2.097(7)−2.128(6)	2.094(3)−2.121(2)	2.097(5)−2.111(4)	2.100(4)−2.115(4)
Re−N	2.435(2)	2.434(5)	2.496(2)	2.410(4)	2.427(3)
			Bond Angles		
N≡Re−C	96.58(11)−99.66(12)	96.8(2)−98.7(2)	96.41(10)−100.78(10)	98.3(2)−101.32(19)	98.47(14)−100.31(14)
N≡Re−N	176.15(10)	176.37(19)	175.82(9)	176.83(17)	178.48(14)

Table 2. Spectroscopic and Photophysical Data of the Complexes in the Crystalline Phase at 296 and 80 K

	296 K			80 K	
	λ_{em}/nm	Φ_{em}	τ_{em}/μs	λ_{em}/nm	τ_{em}/μs
1[a]	569, 720	<0.01	0.35(61), 1.2(35), 7.6(4)	721	0.29(52), 3.3(17), 14(31)
2	535	0.75	54	507, 534, 553, 564	120[b]
2-Dim	532		48	507, 534, 554, 565	120[b]
3	536	0.65	55	514, 540, 567	121(76), 192(24)
4	544	0.70	52	521, 547, 576	166
5	561	<0.01	0.023(58), 0.067(40), 0.35(1), 2.6(1)	515, 541, 563, 571, 592	29[b]
5-Dim	561	<0.01	0.011(18), 0.044(40), 0.24(32), 0.68(10)	514, 542, 564, 574, 593	2.2(10), 20(44), 55(46)[b]
6	537	0.65	52	514, 540, 567	97(84), 198(16)

[a]Reference 49. [b]At 77 K. [c]Parenthesis denotes % components.

(nitrido)≡Re−N(aromatic) angles are almost linear [175.82(9)−178.48(14)°]. The Re−N(aromatic) bond distances are in the range 2.410(4)−2.496(2) Å, which is significantly long because of the trans influence of the nitrido ligand, while the distances are small compared to those in $[ReN(CN)_4L]^{2-}$ (L = six-membered N-heterocyclic ligand) [2.45(1)−2.589(5) Å].[58] This difference may be due to the steric hindrance because the five-membered aromatic ring is sterically less hindered than the six-membered ring. The complex anions in **2** and **5** and the anions in **3** and **6** have very similar geometries, respectively. In **5**, a noncoordinating Him is involved per complex anion and the N−H···N hydrogen bond is formed between the nitrogen atoms in the coordinate Him and that in the noncoordinate Him [N7···N8, 2.804(6) Å]. The noncoordinate Him interacts with the $[ReN(CN)_4]^{2-}$ unit through the N−H···N hydrogen bond to the nitrogen atom of the cyanido [N3···N9, 2.993(7) Å] and the C−H···N bond to the nitrido atom [N1···C9, 3.264(8) Å] and to the cyanido [N5···C10, 3.438(8) Å]. In addition, the C−H···N interaction is shown between the nitrido atom and a phenyl ring of PPh_4^+ [N1···C26, 3.369(8) Å]. In **6**, a noncoordinating Mim is included per complex anion, while there is no hydrogen bonding interaction between the coordinate and noncoordinate Mim molecules. The noncoordinate Mim interacts with the nitrido atom of the complex unit by the C−H···N bond [N1···C12, 3.271(6) Å] and with the cyanide ligand by the C−H···N bond [N5···C10, 3.344(5) Å, N3···C9, 3.384(6) Å]. The C−H···N interactions are formed between the nitrido atom and phenyl rings of PPh_4^+ ions [N1···C22, 3.316(5) Å; N1···C46, 3.494(5) Å]. In **2** and **3**, the weak interactions show as the O−H···N hydrogen bonds among water molecules and the nitrogen atoms of the cyanido ligands [O1···N3, 2.973(5) Å; O2···N3, 2.958(4) Å; O3···N4, 2.853(4) Å for **2** and O1···N4, 2.864(8) Å; O2···N3, 2.930(6) Å; O3···N3, 2.89(1) Å for **3**] and as the N−H···N bond between the coordinate imidazole and the cyanido [N5···N7, 2.854(4) Å] for **2**. Furthermore, the interaction is formed between the nitrido and a carbon atom of a PPh_4^+ ion [N1···C46, 3.276(5) Å for **2** and N1···C43, 3.39(1) Å for **3**]. In **4**, the weak interactions show as the N−H···N and C−H···N bonds between the pyrazole and cyanido [N5···N7, 2.955(4) Å and N5···C7, 3.133(4) Å] and C−H···N bonds between the pyrazole and CH_3CN [C6···N8, 3.268(4) Å]. Moreover, the interactions are formed between the nitrido and carbon atoms of PPh_4^+ ions [N1···C18, 3.385(4) Å and N1···C35, 3.599(3) Å].

Spectroscopic and Photophysical Properties. UV−vis diffuse reflectance spectra of the new complexes were measured in the solid states. Figure S2 in the Supporting Information exhibits the spectra. The complexes show the bands at 405−418 nm. The peak maximum wavelengths are similar to those observed for the six-coordinate tetracyanidonitridorhenium(V) complexes, $[ReN(CN)_4L]^{2-}$ (L = pyridine, MeOH, and acetone).[49,58] The band can be ascribed to the transition $(d_{xy})^2 \rightarrow (d_{xy})^1(d_{\pi^*})^1$ ($d_{\pi^*} = d_{xz}, d_{yz}$) with $p_\pi(N^{3-})-d_\pi$ overlap.[49−58] This electronic transition between the highest energy occupied molecular orbital and lowest energy unoccupied molecular orbital is well characterized in d^2 nitridorhenium(V) complexes.[49−58] The spectroscopic and photophysical data of the complexes in the crystalline phase are shown in Table 2. The emission spectra in the crystalline phase at 296 K are shown in Figures 3 and 4. The complexes, **2**, **3**, **4**, and **6**, are highly photoemissive with the Φ_{em} values being 0.65−0.75. The τ_{em} values (52−55 μs) of these complexes indicate that the emissive excited state is a spin triplet state. Emission spectra at low temperature were measured to investigate further the excited state characters of the complexes. Figures 5 and 6 show the emission spectra of the complexes at 80 K in the crystalline phase. All of the complexes show vibronic progressions with ca. 1000 cm^{-1}, whose value corresponds to the $\nu_{Re\equiv N}$ stretching band frequencies. The emission spectra are typical for the luminescence of a nitridorhenium(V) complex.[49−58] From these results, we assigned the emissive excited state of **2**, **3**, **4**, and **6** to $^3[(d_{xy})^1(d_{xz}$ or $d_{yz})^1]$ with the $p_\pi(N^{3-})-d_\pi$ overlap.

DOI: 10.1021/acsomega.9b02749
ACS Omega 2019, 4, 21251−21259

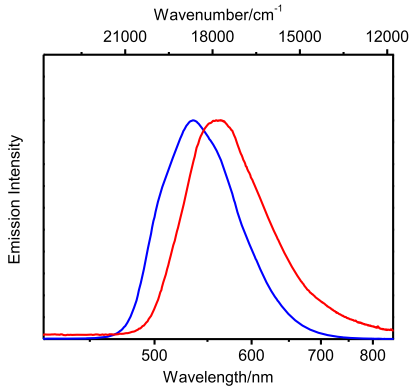

Figure 3. Emission spectra of **2** (blue) and **5** (red) in the crystalline state at 296 K.

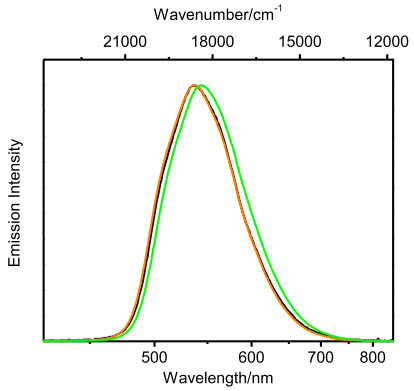

Figure 4. Emission spectra of **3** (black), **4** (green), and **6** (orange) in the crystalline states at 296 K.

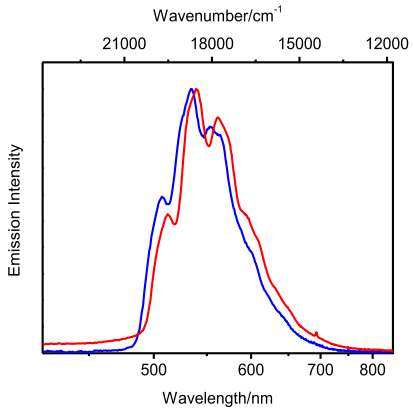

Figure 5. Emission spectra of **2** (blue) and **5** (red) in the crystalline state at 80 K.

The temperature (T) dependences of the emission spectrum and the τ_{em} value of **2** in the crystalline phase were studied in the T range, 80 < T < 296 K as the data were shown in Figure S3 and Table S2 in the Supporting Information. To the best of our knowledge, this is the first demonstration of the T-dependent emission spectrum and τ_{em} of a nitridorhenium(V) complex. As seen in Figure S3, **2** shows the clear vibronic progressions upon cooling, while the emission maximum wavelength is almost insensitive to T. The complex, **2**, exhibits single exponential emission decay irrespective of T and the τ_{em} value increased with decreasing T in 120 < T < 296 K, while it was almost constant at 118−122 μs below 120 K. The rate

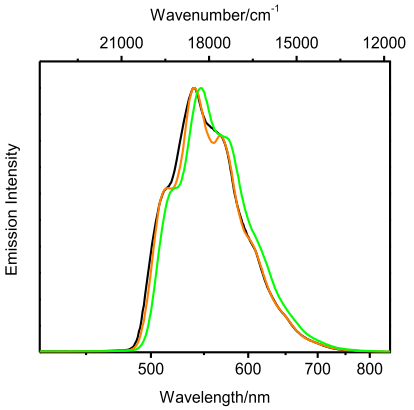

Figure 6. Emission spectra of **3** (black), **4** (green), and **6** (orange) in the crystalline states at 80 K.

constant (k) of **2** evaluated as $k = 1/\tau_{em}$ is 1.86×10^4 s^{-1} at 296 K and 8.2×10^3 s^{-1} at 80 K, respectively. It is known that the k value of $[Ru(2,2'\text{-bipyridine})_3]^{2+}$ in MeOH/EtOH at room temperature decreases significantly with decreasing T from 8.7×10^5 s^{-1} at 296 K to $1.8–2.0 \times 10^5$ s^{-1} at 77 K because thermal deactivation of the emissive excited state of the complex through the upper-energy-lying metal-centered excited state is suppressed at lower temperature.[62] The small variation of the k value with T and the high Φ_{em} value of **2** will be due to almost no contribution of thermal activation to the nonradiative metal-centered state to excited state decay of **2**. Figure 3 also shows the emission spectrum of **5** in the crystalline phase and the relevant spectroscopic/photophysical data are included in Table 2. Although the coordination geometries of **2** and **5** are very similar with each other, the large differences in the λ_{em}, τ_{em}, and Φ_{em} values were observed between those of **2** (λ_{em} = 535 nm, τ_{em} = 54 μs, Φ_{em} = 0.75) and **5** (λ_{em} = 561 nm, weighted average τ_{em} = 0.070 μs, Φ_{em} < 0.01). In particular, the Φ_{em} value of **5** is significantly smaller than those of **2** and the other new complexes. The spectral feature showing vibronic progressions of **5** is very similar to **2** at 80 K. Therefore, the emissive excited state of **5** is assignable to $^3[(d_{xy})^1(d_{xz}$ or $d_{yz})^1]$ with the $p_\pi(N^{3-})–d_\pi$ overlap, and the weak luminescence of **5** is the result of quenching of the emissive excited state of the complex. In the Mim coordinate complexes, both **3** and **6** showed almost comparable spectroscopic and photophysical properties: λ_{em} = 536 nm, τ_{em} = 55 μs, and Φ_{em} = 0.65 for **3** and λ_{em} = 537 nm, τ_{em} = 52 μs, and Φ_{em} = 0.65 for **6**. The Φ_{em} and τ_{em} data observed for **2** and **5** are, thus, in sharp contrast to those of **3** and **6**. As described in the part of X-ray crystallography, the hydrogen bonding interactions present between the coordinate and free imidazole molecules and between the nitrido and free imidazole participate in **5**, although the coordination geometry around the rhenium atoms in **5** is similar to that in **2**. The C–H···N bonds at the nitrido with PPh_4^+ and Mim, and the O–H···N hydrogen bonding interactions at the nitrogen atom(s) of the cyanido with solvent molecules are less effective to the emission quenching because these interactions exist in the crystals of strongly luminescent **2**, **3**, and **6**. For investigation on influence of the N–H···N interaction between coordinate and noncoordinate Him molecules, the tetracyanidonitridorhenium(V) complexes with imidazole-d_5 (Dim) molecule(s), **2-Dim** and **5-Dim**, were prepared by the similar reactions to the synthetic procedures to **2** and **5**

DOI: 10.1021/acsomega.9b02749
ACS Omega 2019, 4, 21251−21259

except for using Dim and deuterated solvents: D_2O for **2**-Dim and CD_2Cl_2/diethylether-d_{10} for **5-Dim**, respectively. The emission spectral and photophysical data of **2-Dim** and **5-Dim** in crystalline phase are also listed in Table 2. The λ_{em} and τ_{em} values of **2-Dim** at both 296 and 80 K are similar to those of **2**, as shown in Supporting Information, Figures S4 and S5. These results indicate that the deuterated ligand gives almost no influence to the excited state character and luminescence properties of **2**. In **5-Dim** and **5**, the emission spectra and the λ_{em} values are similar to each other, while the τ_{em} values of **5** and **5-Dim** in the crystalline phase are different at both 296 and 80 K. The weighted average value of τ_{em} for **5**-Dim (0.16 μs) are longer than that for **5** (0.070 μs) at 296 K. The results suggest that the deuterated ligand in **5-Dim** is hardly contribute to the radiative process while that influences significantly nonradiative decay of the excited states of **5** and **5-Dim**. Therefore, the weak luminescence from **5** is attributed to excited-state deactivation by vibronic relaxation through the N−H···N hydrogen interactions. The longer emission lifetime of **5-Dim** compared to that of **5** would be due to suppression of excited-state quenching by the slow vibration of the N−D···N hydrogen bond compared to that of the N−H···N hydrogen bond. As the noncoordinate Him interacts with the nitrido by the C−H···N bond, the bond may be also involved in the luminescence quenching in **5**.

Luminescence Intensity Change by Solvent-Free Reactions and Exposure of Water. Scheme 1 summarizes the reactions with luminescence intensity change by coordination/dissociation of the Re−N(aromatic) coordination bond and the formation/dissociation of the N−H···N hydrogen bond on the basis of solvent-free reactions and exposure of water. The solid mixture of **2** and 1 mol equiv of Him was mechanically ground on an alumina mortar at room temperature. The bright yellow-green luminescence of **2** gradually disappeared to give **5**. Complex **5** was also afforded by the mechanochemical reaction of **1** with 2 mol equiv of Him at room temperature. Figure 7 shows the luminescence intensity change during the mechanochemical reaction of the solid sample of **1** with 2 mol equiv of Him. The IR spectra and powder X-ray diffraction patterns of the obtained solids by these reactions are identical with that of **5** as shown in Supporting Information, Figures S1 and S6.

Scheme 1. Interconversions among 1, 2, and 5 by Solvent-Free Reactions and Exposure of Water

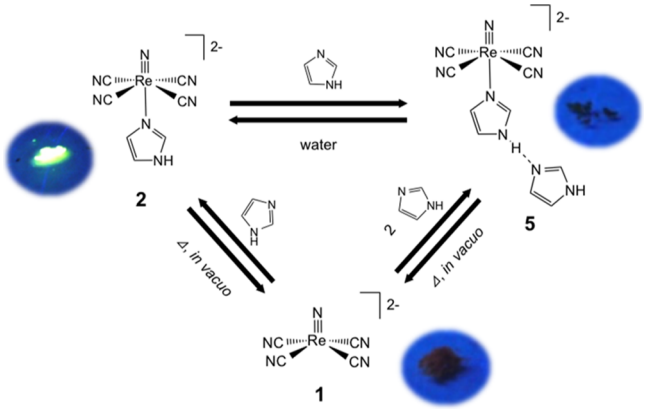

The significant luminescence intensity change induced by the mechanochemical reaction of **2** with one mole ratio of Him is responsible for the large Φ_{em} difference between **2** and **5**. During the solvent-free reaction of **1** to produce **5**, bright yellow-green luminescence appeared upon grinding (the picture in the middle of Figure 7). As the Φ_{em} value of five-coordinate **1** is very small, this observation suggests that coordination of Him at the axial site of **1** gives the six-coordinate complex $[ReN(CN)_4Him]^{2-}$. By continuing grinding, a noncoordinating Him molecule is positioned at the site with the N−H···N hydrogen bond to give the weak luminescent complex, **5**. The mechanochemical reaction of **1** with 1 mol equiv of Him gave a yellow-green luminescent solid. The X-ray powder diffraction of the solid indicates the existence of **2** along with an unidentified substance. The unidentified complex might be $(PPh_4)_2[ReN(CN)_4Him]$ with a crystal system different from that of **2**. When one drop of water was placed on a crystal of **5** under UV irradiation, almost the nonluminescent crystal gradually exhibited yellow-green photoemission as the water spread around the crystal as shown in Figure 8 and Movie 1 in the Supporting Information. The emission spectrum of the crystal agrees well with that of **2** in the crystalline phase. After the microcrystalline sample of **5** being soaked in water for 3.5 h, the IR spectrum and powder X-ray diffraction pattern of the solid changed to those of **2** (Figures S1 and S7), and the signal integrated intensity ratio of Him and $(PPh_4)^+$ is 1:2 in the ^{1}H NMR spectrum in CD_3CN (Figure S8). These results suggest that noncoordinating Him is eliminated by soaking the solid in water and three H_2O molecules are incorporated to give **2**. When **5** was suspended in 0.7 mL of D_2O, ca. 3% of the complex was dissolved during the reaction; the ^{1}H NMR spectrum of this solution was used to obtain the signal intensity ratio of $(PPh_4)^+$ to the DSS

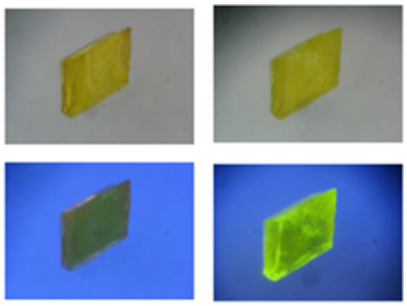

Figure 8. Crystal of **5** (upper left) and under UV irradiation (lower left); the crystal with an added drop of water (upper right) and the wet crystal under UV irradiation (lower right).

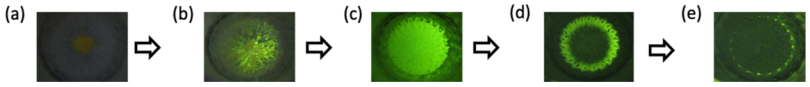

Figure 7. Luminescence intensity change during the mechanochemical reaction of **1** with Him in a 1:2 mole ratio in the solid state at room temperature. (a) Before the reaction, (b) after 1 min, (c) after 3 min, (d) after 8 min, (e) after 15 min. The pictures were taken under UV irradiation.

DOI: 10.1021/acsomega.9b02749
ACS Omega 2019, 4, 21251−21259

internal reference. Therefore, the conversion of **5** to **2** may proceed through the process of the dissolution of the complex in water. When the microcrystalline solid of **6** was placed in a small amount of water and the mixture was allowed to stand for 3.5 h, the IR spectrum and powder X-ray diffraction pattern changed to those of **3** (Figures S1 and S9). Therefore, elimination of the noncoordinating Mim molecule in **6** proceeds by exposure of water to give **3**, although the intense luminescence remains through the reaction because the Φ_{em} values of **3** and **6** are similar to each other.

Vacuum elimination of Him from **2** or **5** was performed to achieve interconversion between the five- and six-coordinate complexes. Figures S10 and S11 exhibit the thermal gravimetric curve for **2** and **5**, respectively. The thermal gravimetric analysis of **2** shows loss of water from 30 to 70 °C and large weight loss above 170 °C, and that of **5** exhibits weight loss above 150 °C. When the microcrystalline sample of **2** was subjected to vacuum at 185 °C, photoemission gradually weakened. After the vacuum elimination reaction for 6 days, no yellow-green luminescence was visible by naked eyes. In the ^{1}H NMR spectrum, the signals of Him are not appeared in the obtained complex. The IR spectrum of the complex agrees to that of **1** as shown in Figure S1. Therefore, conversion of **2** to **1** was carried out under vacuum at 185 °C. The complex **1** was also produced from **5** by vacuum elimination of Him at 185 °C. As shown in Figure S12, the X-ray powder diffraction patterns of the obtained complexes were not agreed with that of **1** which was prepared from the vacuum elimination reaction of $(PPh_4)_2[ReN(CN)_4MeOH]$. This would be because the molecular packing of **1** in the solid depends on the starting material in the vacuum elimination of the ligand at the axial site.

CONCLUSIONS

The tetracyanidonitridorhenium(V) complexes with five-membered N-heteroaromatic ligands were synthesized and their spectroscopic and photophysical properties were characterized. All of the complexes in the present study showed high-emission quantum yield, except for $(PPh_4)_2[ReN(CN)_4Him]\cdot Him$. The nature of the emissive excited state was characterized to $^3[(d_{xy})^1(d_{xz}$ or $d_{yz})^1]$ with the $p_\pi(N^{3-})-d_\pi$ overlap. The temperature dependence of emission lifetimes was measured at first time in the nitridorhenium(V) complex using$(PPh_4)_2[ReN(CN)_4Him]$. The bright yellow-green luminescence intensity change was accomplished by the solid-based reactions of the complexes involving changes in the coordination number and in the environment around the complex. The results demonstrated that the luminescence intensity change was controlled by the formation/dissociation of the weak bond in the solid state.

EXPERIMENTAL SECTION

Materials. All commercially available reagents were used as received. $(PPh_4)_2[ReN(CN)_4]$ (**1**) was prepared according to the literature procedure.[49]

Syntheses of the Complexes. *$(PPh_4)_2[ReN(CN)_4Him]\cdot 3H_2O$ (2).* **Method 1**: Him (212 mg, 3.12 mmol) and **1** (121 mg, 0.123 mmol) were dissolved in 2 mL hot water. The solution was cooled to room temperature to give yellow crystals. The crystals were washed with cold water and dried under vacuum. Yield: 122 mg (91.2%). Anal. Calcd for $C_{55}H_{44}N_7P_2Re\cdot 3H_2O$: C, 59.77; H, 4.56; N, 8.87%. Found: C, 59.82; H, 4.49; N, 8.76%. ^{1}H NMR in CD_3CN/ppm: 6.92 (s, 2H, Him), 7.61 (s, 1H, Him), 7.64−7.94 (40H, PPh_4^+), 10.09 (br, 1H, Him). UV−vis/nm in the solid state: 408. IR (KBr pellet)/cm^{-1}: 2129 ($\nu_{C\equiv N}$), 2115 ($\nu_{C\equiv N}$), 2105 ($\nu_{C\equiv N}$), 2098 ($\nu_{C\equiv N}$).

Method 2: The microcrystalline solid of $(PPh_4)_2[ReN(CN)_4Him]\cdot Him$ (**3**) (22.3 mg, 0.0199 mmol) was placed in small amounts of water (∼0.1 mL) and allowed to stand for 3.5 h. The solid was collected and washed with small amounts of water and then dried under vacuum. Yield: 21.1 mg (95.8%).

Preparation of $(PPh_4)_2[ReN(CN)_4Mim]\cdot 3H_2O$ (3). **Method 1:** Mim (110 mg, 1.33 mmol) and **1** (100 mg, 0.102 mmol) were dissolved in 4 mL of hot water. The solution was cooled to room temperature to give yellow crystals. The crystals were washed with water and then dried under vacuum. Yield: 93.1 mg (85.7%). Anal. Calcd for $C_{56}H_{46}N_7P_2Re\cdot 3H_2O$: C, 60.10; H, 4.68; N, 8.76%. Found: C, 60.23; H, 4.59; N, 8.81%. ^{1}H NMR in CD_3CN/ppm: 3.59 (s, 3H, $-CH_3$), 6.77 (dd, 1H, Mim), 6.94 (d, 1H, Mim), 7.47 (s, 1H, Mim), 7.64−7.93 (40H, PPh_4). UV−vis/nm in the solid state: 415. IR (KBr pellet)/cm^{-1}: 2126 ($\nu_{C\equiv N}$), 2113 ($\nu_{C\equiv N}$), 2102 ($\nu_{C\equiv N}$), 2095 ($\nu_{C\equiv N}$).

Method 2: The microcrystalline solid of $(PPh_4)_2[ReN(CN)_4Mim]\cdot Mim$ (**6**) (22.5 mg, 0.0196 mmol) was placed in small amounts of water and allowed to stand for 3.5 h. The resultant solid was collected and washed with small amounts of water, and then dried under vacuum. Yield: 21.3 mg (97.0%).

Preparation of $(PPh_4)_2[ReN(CN)_4pyz]$ (4). **1** (40.3 mg, 0.0410 mmol) and pyz (152.5 mg, 2.24 mmol) were dissolved in 4 mL CH_2Cl_2, followed by addition of a 4 mL layer of Et_2O. The solution was left for several days, resulting in the formation of yellow crystals, which were filtered and washed with Et_2O. Yield: 38.8 mg (85.7%). Anal. Calcd for $C_{55}H_{44}N_7P_2Re\cdot 2.5H_2O$: C, 60.26; H, 4.51; N, 8.94%. Found: C, 60.15; H, 4.52; N, 9.22%. ^{1}H NMR in CD_3CN/ppm: 6.23 (t, 1H, pyrazole), 7.53 (d, 2H, pyrazole), 7.64−7.93 (40H, PPh_4^+). UV−vis/nm in the solid state: 412. IR (KBr pellet)/cm^{-1}: 2128 ($\nu_{C\equiv N}$), 2106 ($\nu_{C\equiv N}$), 2098 ($\nu_{C\equiv N}$).

Preparation of $(PPh_4)_2[ReN(CN)_4Him]\cdot Him$ (5). **Method 1:** Him (177 mg, 2.59 mmol) and **1** (100 mg, 0.102 mmol) were dissolved in 10 mL CH_2Cl_2, followed by addition of a 10 mL layer of Et_2O. The solution was left for several days, resulting in the formation of yellow crystals, which were filtered and washed with Et_2O. Yield: 102 mg (89.1%). Anal. Calcd for $C_{58}H_{48}N_9P_2Re$: C, 62.24; H, 4.32; N, 11.26%. Found: C, 62.38; H, 4.27; N, 11.36%. ^{1}H NMR in CD_3CN/ppm: 6.94 (s, 4H, Him), 7.60 (s, 2H, Him), 7.64−7.95 (40H, PPh_4^+), 10.31 (br, 2H, Him) UV−vis/nm in the solid state: 405. IR (KBr pellet)/cm^{-1}: 2103 ($\nu_{C\equiv N}$), 2089 ($\nu_{C\equiv N}$), 2124 ($\nu_{C\equiv N}$).

Method 2: Him (10.8 mg, 0.158 mmol) and **1** (77.8 mg, 0.0791 mmol) were ground in an alumina mortar using the automated mill (Nitto, ALM-90DM) for 30 min. Yield: 73.1 mg (82.5%).

Method 3: Him (4.83 mg, 0.0709 mmol) and **2** (78.4 mg, 0.0709 mmol) were ground in an alumina mortar using the automated mill (Nitto, ALM-90DM) for 20 min. Yield: 67.7 mg (85.3%).

Conversion from 2 to 1. **2** (173 mg, 0.156 mmol) was heated at 185 °C for 6 days under vacuum. Yield: 145 mg (94.6%). Anal. Calcd for $C_{52}H_{40}N_5P_2Re\cdot 4.5H_2O$: C, 58.69; H, 4.64; N, 6.58%. Found: C, 58.62; H, 4.34; N, 6.65%. IR (KBr pellet) and ^{1}H NMR (CD_3CN) spectra agreed well with those previously reported.[49]

DOI: 10.1021/acsomega.9b02749
ACS Omega 2019, 4, 21251−21259

Conversion from 5 to 1. **5** (84.6 mg, 0.0756 mmol) was heated at 185 °C for 8 days under vacuum. Yield: 71.2 mg (95.9%). IR (KBr pellet) and ^{1}H NMR (CD_3CN) spectra agreed well with those previously reported.[49]

*Preparation of $(PPh_4)_2$[ReN(CN)$_4$Mim]·Mim (**6**).* Mim (400 μL, 5.02 mmol) and **1** (32.4 mg, 0.0330 mmol) were dissolved in 1 mL CH_2Cl_2, followed by addition of a 9 mL layer of Et_2O on the solution. The solution was allowed to stand for several days, resulting in formation of yellow crystals, which were filtered and washed with Et_2O. Yield: 34.5 mg (84.8%). Anal. Calcd for $C_{60}H_{52}N_9P_2Re{\cdot}CH_2Cl_2$: C, 59.46; H, 4.42; N, 10.23%. Found: C, 59.32; H, 4.58; N, 10.23%. ^{1}H NMR in CD_3CN/ppm: 3.64 (s, 6H, Mim), 6.82 (t, 2H, Mim), 6.93 (t, 2H, Mim), 7.45 (t, 2H, Mim), 7.60−7.90 (40H, PPh_4^+). UV−vis/nm in the solid state: 418. IR (KBr pellet)/cm^{-1}: 2133 ($\nu_{C\equiv N}$), 2110 ($\nu_{C\equiv N}$), 2102 ($\nu_{C\equiv N}$).

X-ray Crystallography. The single-crystal X-ray data were collected at −103 °C on a Rigaku RAXIS diffractometer with graphite-monochromated Mo Kα radiation. The crystal structures were solved by SHELXT version 2014.[63] Atomic coordinates and thermal parameters of nonhydrogen atoms were calculated by a full-matrix least-squares method using SHELXL version 2017.[64] Calculations were performed using CrystalStructure 4.2.4.

Physical Measurements. ^{1}H NMR spectra were recorded on a JEOL ECS 400 MHz spectrometer. All peaks were referred to the proton signal of $Si(CH_3)_4$ at δ = 0.00. Solid-state reflectance UV−vis spectra were measured by a JASCO V-550 spectrophotometer equipped with an integration sphere, and a sample was placed between two silica glass plates. IR spectra were recorded on a JASCO FTIR-4100. X-ray powder diffraction patterns were collected on a RIGAKU Rint 2000 diffractometer using Cu Kα radiation (λ = 1.54178 Å) with a scan rate of 1°/min($5 \leq 2\theta \leq 50°$). Corrected emission spectra excited at 400 nm were measured by an absolute emission quantum yield measurement system (Hamamatsu C9920-02) composed of an integrating sphere, a multichannel photodetector (Hamamatsu Photonics, PMA-12), and a xenon lamp as an excitation light source. For emission lifetime measurements, a solid sample was placed between two nonfluorescent glass plates. A pulsed Nd^{3+}:YAG laser (Lotis TII Ltd., 355 nm, fwhm ∼6 ns or continuum, 355 nm, fwhm 4−6 ns) was used as an excitation light source. The emission lifetime was measured by using a streak camera (Hamamatsu Photonics, C4334) or a photomultiplier tube (Hamamatsu, R928) monitored by a digital oscilloscope (IWATSU, DS-5532A). A liquid N_2 cryostat (DN1704 optical Dewar and 3120 temperature controller, Oxford Instruments) was used to control the sample temperature. The pictures of luminescence were taken under irradiation of UV light at 365 nm using a UV lamp (Vilber, VL-6.LC).

■ ASSOCIATED CONTENT

Supporting Information

The Supporting Information is available free of charge on the ACS Publications website at DOI: 10.1021/acsomega.9b02749.

Crystallographic data, temperature dependence of emission lifetimes and phosphorescent rate constants of **2**, IR spectra, solid-state reflectance spectra, temperature dependence of emission spectra for **2**, emission spectra of **2-Dim** and **5-Dim** at 296 and 80 K, powder X-ray diffractions, ^{1}H NMR spectra for **5**, Thermogravimetric curves of **2** and **5** (PDF)

Luminescent intensity change of **5** by exposure of water under a UV lamp (MP4)

Crystallographic files for **2**, **3**, **4**, **5**, and **6** (CIF)

■ AUTHOR INFORMATION

Corresponding Author

*E-mail: tyoshi@rirc.osaka-u.ac.jp.

ORCID

Akitaka Ito: 0000-0002-0893-5535

Eri Sakuda: 0000-0001-9882-7628

Takashi Yoshimura: 0000-0002-9216-9043

Notes

The authors declare no competing financial interest.

■ REFERENCES

(1) Lee, Y.-A.; Eisenberg, R. Luminescence Tribochromism and Bright Emission in Gold(I) Thiouracilate Complexes. *J. Am. Chem. Soc.* **2003**, *125*, 7778−7779.

(2) Ito, H.; Saito, T.; Oshima, N.; Kitamura, N.; Ishizaka, S.; Hinatsu, Y.; Wakeshima, M.; Kato, M.; Tsuge, K.; Sawamura, M. Reversible Mechanochromic Luminescence of [$(C_6F_5Au)_2$(μ-1,4-Diisocyanobenzene)]. *J. Am. Chem. Soc.* **2008**, *130*, 10044−10045.

(3) Balch, A. L. Dynamic crystals: visually detected mechanochemical changes in the luminescence of gold and other transition-metal complexes. *Angew. Chem., Int. Ed.* **2009**, *48*, 2641−2644.

(4) Osawa, M.; Kawata, I.; Igawa, S.; Hoshino, M.; Fukunaga, T.; Hashizume, D. Vapochromic and Mechanochromic Tetrahedral Gold(I) Complexes Based on the 1,2-Bis(diphenylphosphino)-benzene Ligand. *Chem.—Eur. J.* **2010**, *16*, 12114−12126.

(5) Perruchas, S.; Le Goff, X. F.; Maron, S.; Maurin, I.; Guillen, F.; Garcia, A.; Gacoin, T.; Boilot, J.-P. Mechanochromic and Thermochromic Luminescence of a Copper Iodide Cluster. *J. Am. Chem. Soc.* **2010**, *132*, 10967−10969.

(6) Tsukuda, T.; Kawase, M.; Dairiki, A.; Matsumoto, K.; Tsubomura, T. Brilliant reversible luminescent mechanochromism of silver(I) complexes containing o-bis(diphenylphosphino)benzene and phosphinesulfide. *Chem. Commun.* **2010**, *46*, 1905−1907.

(7) Tzeng, B.-C.; Chang, T.-Y.; Sheu, H.-S. Reversible Phase Transformation and Luminescent Mechanochromism of ZnII-Based Coordination Frameworks Containing a Dipyridylamide Ligand. *Chem.—Eur. J.* **2010**, *16*, 9990−9993.

(8) Ni, J.; Zhang, X.; Qiu, N.; Wu, Y.-H.; Zhang, L.-Y.; Zhang, J.; Chen, Z.-N. Mechanochromic Luminescence Switch of Platinum(II) Complexes with 5-Trimethylsilylethynyl-2,2′-bipyridine. *Inorg. Chem.* **2011**, *50*, 9090−9096.

(9) Ni, J.; Zhang, X.; Wu, Y.-H.; Zhang, L.-Y.; Chen, Z.-N. Vapor- and Mechanical-Grinding-Triggered Color and Luminescence Switches for Bis(σ-fluorophenylacetylide) Platinum(II) Complexes. *Chem.—Eur. J.* **2011**, *17*, 1171−1183.

(10) Choi, S. J.; Kuwabara, J.; Nishimura, Y.; Arai, T.; Kanbara, T. Two-step changes in luminescence color of Pt(II) complex bearing an amide moiety by mechano- and vapochromism. *Chem. Lett.* **2012**, *41*, 65−67.

(11) Kumpfer, J. R.; Taylor, S. D.; Connick, W. B.; Rowan, S. J. Vapochromic and mechanochromic films from square-planar platinum complexes in polymethacrylates. *J. Mater. Chem.* **2012**, *22*, 14196−14204.

(12) Tzeng, B. C.; Chang, T. Y.; Wei, S. L.; Sheu, H. S. Reversible Phase Transformation and Mechanochromic Luminescence of ZnII-Dipyridylamide-Based Coordination Frameworks. *Chem.—Eur. J.* **2012**, *18*, 5105−5112.

(13) Zhang, X.; Wang, J.-Y.; Ni, J.; Zhang, L.-Y.; Chen, Z.-N. Vapochromic and Mechanochromic Phosphorescence Materials

DOI: 10.1021/acsomega.9b02749
ACS Omega 2019, 4, 21251−21259

Based on a Platinum(II) Complex with 4-Trifluoromethylphenylacetylide. *Inorg. Chem.* **2012**, *51*, 5569−5579.
(14) Kawaguchi, K.; Seki, T.; Karatsu, T.; Kitamura, A.; Ito, H.; Yagai, S. Cholesterol-aided construction of distinct self-organized materials from a luminescent gold(I)-isocyanide complex exhibiting mechanochromic luminescence. *Chem. Commun.* **2013**, *49*, 11391−11393.
(15) Shan, X.-C.; Jiang, F.-L.; Zhang, H.-b.; Qian, X.-Y.; Chen, L.; Wu, M.-Y.; Al-Thabaiti, S. A.; Hong, M.-C. A solid AND logic stimuli-responsive material with bright nondestructive performance designed by sensitive cuprophilicity. *Chem. Commun.* **2013**, *49*, 10227−10229.
(16) Shan, X.-C.; Zhang, H.-B.; Chen, L.; Wu, M.-Y.; Jiang, F.-L.; Hong, M.-C. Multistimuli-Responsive Luminescent Material Reversible Switching Colors via Temperature and Mechanical Force. *Cryst. Growth Des.* **2013**, *13*, 1377−1381.
(17) Zhang, X.; Chi, Z.; Zhang, Y.; Liu, S.; Xu, J. Recent advances in mechanochromic luminescent metal complexes. *J. Mater. Chem. C* **2013**, *1*, 3376−3390.
(18) Berenguer, J. R.; Fernández, J.; Gil, B.; Lalinde, E.; Sánchez, S. Reversible Binding of Solvent to Naked Pb(II) Centers in Unusual Homoleptic Alkynyl-Based Pt_2Pb_2 Clusters. *Chem.—Eur. J.* **2014**, *20*, 2574−2584.
(19) Han, A.; Du, P.; Sun, Z.; Wu, H.; Jia, H.; Zhang, R.; Liang, Z.; Cao, R.; Eisenberg, R. Reversible Mechanochromic Luminescence at Room Temperature in Cationic Platinum(II) Terpyridyl Complexes. *Inorg. Chem.* **2014**, *53*, 3338−3344.
(20) Jobbágy, C.; Molnár, M.; Baranyai, P.; Deák, A. Mechanochemical synthesis of crystalline and amorphous digold(I) helicates exhibiting anion- and phase-switchable luminescence properties. *Dalton Trans.* **2014**, *43*, 11807−11810.
(21) Krikorian, M.; Liu, S.; Swager, T. M. Columnar Liquid Crystallinity and Mechanochromism in Cationic Platinum(II) Complexes. *J. Am. Chem. Soc.* **2014**, *136*, 2952−2955.
(22) Ni, J.; Wang, Y.-G.; Wang, H.-H.; Pan, Y.-Z.; Xu, L.; Zhao, Y.-Q.; Liu, X.-Y.; Zhang, J.-J. Reversible Dual-Stimulus-Responsive Luminescence and Color Switch of a Platinum Complex with 4-[(2-Trimethylsilyl)ethynyl]-2,2′-bipyridine. *Eur. J. Inorg. Chem.* **2014**, *2014*, 986−993.
(23) Ni, J.; Wang, Y.-G.; Wang, H.-H.; Xu, L.; Zhao, Y.-Q.; Pan, Y.-Z.; Zhang, J.-J. Thermo- and mechanical-grinding-triggered color and luminescence switches of the diimine-platinum(II) complex with 4-bromo-2,2′-bipyridine. *Dalton Trans.* **2014**, *43*, 352−360.
(24) Ni, W.-X.; Qiu, Y.-M.; Li, M.; Zheng, J.; Sun, R. W.-Y.; Zhan, S.-Z.; Ng, S. W.; Li, D. Metallophilicity-Driven Dynamic Aggregation of a Phosphorescent Gold(I)-Silver(I) Cluster Prepared by Solution-Based and Mechanochemical Approaches. *J. Am. Chem. Soc.* **2014**, *136*, 9532−9535.
(25) Wen, T.; Zhou, X.-P.; Zhang, D.-X.; Li, D. Luminescent Mechanochromic Porous Coordination Polymers. *Chem.—Eur. J.* **2014**, *20*, 644−648.
(26) Zhang, S.-T.; Li, T.-R.; Wang, B.-D.; Yang, Z.-Y.; Liu, J.; Wang, Z.-Y.; Dong, W.-K. A new cyclic supramolecular Zn(II) complex derived from a N_2O_2 oxime chelate ligand with luminescence mechanochromism. *Dalton Trans.* **2014**, *43*, 2713−2717.
(27) Aliprandi, A.; Genovese, D.; Mauro, M.; De Cola, L. Recent Advances in Phosphorescent Pt(II) Complexes Featuring Metallophilic Interactions: Properties and Applications. *Chem. Lett.* **2015**, *44*, 1152−1169.
(28) Baranyai, P.; Marsi, G.; Jobbágy, C.; Domján, A.; Oláh, L.; Deák, A. Mechano-induced reversible colour and luminescence switching of a gold(I)-diphosphine complex. *Dalton Trans.* **2015**, *44*, 13455−13459.
(29) Chen, K.; Nenzel, M. M.; Brown, T. M.; Catalano, V. J. Luminescent Mechanochromism in a Gold(I)-Copper(I) N-Heterocyclic Carbene Complex. *Inorg. Chem.* **2015**, *54*, 6900−6909.
(30) Deák, A.; Jobbágy, C.; Marsi, G.; Molnár, M.; Szakács, Z.; Baranyai, P. Anion-, Solvent-, Temperature-, and Mechano-Responsive Photoluminescence in Gold(I) Diphosphine-Based Dimers. *Chem.—Eur. J.* **2015**, *21*, 11495−11508.
(31) Deshmukh, M. S.; Yadav, A.; Pant, R.; Boomishankar, R. Thermochromic and Mechanochromic Luminescence Umpolung in Isostructural Metal-Organic Frameworks Based on Cu_6I_6 Clusters. *Inorg. Chem.* **2015**, *54*, 1337−1345.
(32) Ma, Z.; Wang, Z.; Teng, M.; Xu, Z.; Jia, X. Mechanically Induced Multicolor Change of Luminescent Materials. *ChemPhysChem* **2015**, *16*, 1811−1828.
(33) Seki, T.; Ozaki, T.; Okura, T.; Asakura, K.; Sakon, A.; Uekusa, H.; Ito, H. Interconvertible multiple photoluminescence color of a gold(I) isocyanide complex in the solid state: solvent-induced blue-shifted and mechano-responsive red-shifted photoluminescence. *Chem. Sci.* **2015**, *6*, 2187−2195.
(34) Zhang, X.-P.; Mei, J.-F.; Lai, J.-C.; Li, C.-H.; You, X.-Z. Mechano-induced luminescent and chiroptical switching in chiral cyclometalated platinum(II) complexes. *J. Mater. Chem. C* **2015**, *3*, 2350−2357.
(35) Jobbágy, C.; Baranyai, P.; Marsi, G.; Rácz, B.; Li, L.; Naumov, P.; Deák, A. Novel gold(I) diphosphine-based dimers with aurophilicity triggered multistimuli light-emitting properties. *J. Mater. Chem. C* **2016**, *4*, 10253−10264.
(36) Kobayashi, A.; Hasegawa, T.; Yoshida, M.; Kato, M. Environmentally Friendly Mechanochemical Syntheses and Conversions of Highly Luminescent Cu(I) Dinuclear Complexes. *Inorg. Chem.* **2016**, *55*, 1978−1985.
(37) Penney, A. A.; Sizov, V. V.; Grachova, E. V.; Krupenya, D. V.; Gurzhiy, V. V.; Starova, G. L.; Tunik, S. P. Aurophilicity in Action: Fine-Tuning the Gold(I)-Gold(I) Distance in the Excited State To Modulate the Emission in a Series of Dinuclear Homoleptic Gold(I)-NHC Complexes. *Inorg. Chem.* **2016**, *55*, 4720−4732.
(38) Seki, T.; Jin, M.; Ito, H. Introduction of a Biphenyl Moiety for a Solvent-Responsive Aryl Gold(I) Isocyanide Complex with Mechanical Reactivation. *Inorg. Chem.* **2016**, *55*, 12309−12320.
(39) Seki, T.; Takamatsu, Y.; Ito, H. A Screening Approach for the Discovery of Mechanochromic Gold(I) Isocyanide Complexes with Crystal-to-Crystal Phase Transitions. *J. Am. Chem. Soc.* **2016**, *138*, 6252−6260.
(40) Zhang, X.; Zhu, L.; Wang, X.; Shi, Z.; Lin, Q. Mechano-induced multi-functional optical switches based on chiral cyclometalated platinum(II) complexes. *Inorg. Chim. Acta* **2016**, *442*, 56−63.
(41) Kobayashi, A.; Kato, M. Stimuli-responsive Luminescent Copper(I) Complexes for Intelligent Emissive Devices. *Chem. Lett.* **2017**, *46*, 154−162.
(42) Kwon, E.; Kim, J.; Lee, K. Y.; Kim, T. H. Non-Phase-Transition Luminescence Mechanochromism of a Copper(I) Coordination Polymer. *Inorg. Chem.* **2017**, *56*, 943−949.
(43) Liang, P.; Kobayashi, A.; Hasegawa, T.; Yoshida, M.; Kato, M. Thermal and Mechanochemical Syntheses of Luminescent Mononuclear Copper(I) Complexes. *Eur. J. Inorg. Chem.* **2017**, *2017*, 5134−5142.
(44) Lin, C.-J.; Liu, Y.-H.; Peng, S.-M.; Shinmyozu, T.; Yang, J.-S. Excimer-Monomer Photoluminescence Mechanochromism and Vapochromism of Pentiptycene-Containing Cyclometalated Platinum(II) Complexes. *Inorg. Chem.* **2017**, *56*, 4978−4989.
(45) Damoense, L. J.; Purcell, W.; Leipoldt, J. G. Kinetic study of the reaction between trans-aquanitridotetracyanorhenate(V) and different cyanide species. *Transition Met. Chem.* **1994**, *19*, 619−622.
(46) Mtshali, T. N.; Purcell, W.; Visser, H. G.; Basson, S. S. A crystallographic and kinetic study of the formation of the tricyanonitrido(pyridine-2-carboxylato-κN,κO)rhenate(V) ion, $[ReN(\eta^2\text{-pic})(CN)_3]_2$. *Polyhedron* **2006**, *25*, 2415−2425.
(47) Mtshali, T. N.; Purcell, W.; Visser, H. G.; Basson, S. S. Kinetic study of reaction of $[ReN(H_2O)(CN)_4]^{2-}$ with quinoline-2-carboxylate and pyridine-2,3-dicarboxylate anions. *Transition Met. Chem.* **2008**, *33*, 481−491.
(48) Mtshali, T. N.; Purcell, W.; Visser, H. G.; Basson, S. S. A novel rhenium-aqua structure: the synthesis and structural characterization of $(PPh_4)_4[ReN(H_2O)(CN)_3\text{-}\mu\text{-CN-}ReN(CN)_4]\cdot 5H_2O$. *Transition Met. Chem.* **2008**, *33*, 711−716.

DOI: 10.1021/acsomega.9b02749
ACS Omega 2019, 4, 21251−21259

(49) Ikeda, H.; Yoshimura, T.; Ito, A.; Sakuda, E.; Kitamura, N.; Takayama, T.; Sekine, T.; Shinohara, A. Photoluminescence Switching with Changes in the Coordination Number and Coordinating Volatile Organic Compounds in Tetracyanidonitridorhenium(V) and -technetium(V) Complexes. *Inorg. Chem.* **2012**, *51*, 12065−12074.
(50) Neyhart, G. A.; Bakir, M.; Boaz, J.; Vining, W. J.; Patrick Sullivan, B. Photophysics and photochemistry of rhenium(V)-nitrogen triple bonds. *Coord. Chem. Rev.* **1991**, *111*, 27−32.
(51) Neyhart, G. A.; Seward, K. J.; Boaz, J.; Sullivan, B. P. Luminescent nitridorhenium(V) complexes. *Inorg. Chem.* **1991**, *30*, 4486−4488.
(52) Yam, V. W.-W.; Tam, K.-K.; Lai, T.-F. Syntheses, spectroscopy and electrochemistry of nitridorhenium(V) organometallics. X-ray crystal structure of $[Re^{V}(N)Me_2(PPh_3)_2]$. *J. Chem. Soc., Dalton Trans.* **1993**, 651−652.
(53) Yam, V. W.-W.; Tam, K.-K. Synthesis, spectroscopy and electrochemistry of luminescent $[Re^{V}N\{Ph_2P(CH_2)_2PPh_2\}_2(MeCN)]^{2+}$. *J. Chem. Soc., Dalton Trans.* **1994**, 391−392.
(54) Yam, V. W.-W.; Tam, K.-K.; Cheung, K.-K. Syntheses, electrochemistry, photophysics and photochemistry of nitridorhenium(V) diphosphine complexes and related nitridorhenium(V) organometallics; crystal structure of $[Re^{V}N(C{\equiv}CBut)_2(PPh_3)_2]$. *J. Chem. Soc., Dalton Trans.* **1996**, 1125−1132.
(55) Oetliker, U.; Savoie, C.; Stanislas, S.; Reber, C.; Connac, F.; Beauchamp, A. L.; Stanislas, S.; Connac, F. variation of the luminescence energy from rhenium(V) complexes with oxo and nitrido ligands. *Chem. Commun.* **1998**, 657−658.
(56) Yam, V. W.-W.; Pui, Y. L.; Man-Chung Wong, K.; Cheung, K.-K. Synthesis, structural characterization, photophysics, photochemistry and electrochemistry of nitrido- and trans-dioxo-rhenium(V) complexes with substituted dppe ligands (dppe = bis-(diphenylphosphino)ethane). *Inorg. Chim. Acta* **2000**, *300*−*302*, 721−732.
(57) Bailey, S. E.; Eikey, R. A.; Abu-Omar, M. M.; Zink, J. I. Excited-State Distortions Determined from Structured Luminescence of Nitridorhenium(V) Complexes. *Inorg. Chem.* **2002**, *41*, 1755−1760.
(58) Ikeda, H.; Ito, A.; Sakuda, E.; Kitamura, N.; Takayama, T.; Sekine, T.; Shinohara, A.; Yoshimura, T. Excited-State Characteristics of Tetracyanidonitridorhenium(V) and -technetium(V) Complexes with N-Heteroaromatic Ligands. *Inorg. Chem.* **2013**, *52*, 6319−6327.
(59) Purcell, W.; Potgieter, I. Z.; Damoense, L. J.; Leipolldt, J. S. The crystal structure of tetraphenylphosphonium pentacyanonitridorhenate(V), $(PPh_4)_3[ReN(CN)_5].7H_2O$. *Transition Met. Chem.* **1991**, *16*, 473−475.
(60) Purcell, W.; Damoense, L. J.; Leipoldt, J. G. Chemical structure of the azidonitridotetracyanorhenate(V) ion. *Inorg. Chim. Acta* **1992**, *195*, 217−220.
(61) Mtshali, T. N.; Purcell, W.; Visser, H. G. Tetraphenylphosphonium aquatetracyanonitridorhenate(V) pentahydrate. *Acta Crystallogr., Sect. E: Struct. Rep. Online* **2007**, *63*, m1037−m1038.
(62) Basson, A.; Balzani, V.; Barigelletti, F.; Campagna, S.; Belser, P.; von Zelewsky, A. Ru(II) polypyridine complexes: photophysics, photochemistry, eletrochemistry, and chemiluminescence. *Coord. Chem. Rev.* **1988**, *84*, 85−277.
(63) Sheldrick, G. M. SHELXT - Integrated space-group and crystal-structure determination. *Acta Crystallogr., Sect. A: Found. Adv.* **2015**, *71*, 3−8.
(64) Sheldrick, G. M. Crystal structure refinement with SHELXL. *Acta Crystallogr., Sect. C: Struct. Chem.* **2015**, *71*, 3−8.

DOI: 10.1021/acsomega.9b02749
ACS Omega 2019, 4, 21251−21259